Remote Sensing Applications: Society and Environment 33 (2024) 101106

Contents lists available at ScienceDirect

Remote Sensing Applications: Society and Environment

journal homepage: www.elsevier.com/locate/rsase

Seasonal characteristics of outdoor thermal comfort and residential electricity consumption: A Snapshot in Bangkok Metropolitan Area

Can Trong Nguyen [a, b, *], Ho Nguyen [c, d], Anjar Dimara Sakti [e]

[a] Faculty of Engineering, Prince of Songkla University (Hatyai Campus), Songkhla, 90110, Thailand
[b] Environment Centre, Charles University, Prague, 16000, Czech Republic
[c] Department of Land Management, Dong Thap University, Cao Lanh City, Viet Nam
[d] Institute of Landscape Ecology, University of Münster, Heisenbergstr. 2, 48149, Münster, Germany
[e] Remote Sensing and Geographic Information Sciences Research Group, Faculty of Earth Sciences and Technology, Institut Teknologi Bandung, Bandung, Indonesia

ARTICLE INFO

Keywords:
Building density
Outdoor thermal comfort
Residential electricity consumption
Seasonal characteristics
Thermal vulnerability

ABSTRACT

Outdoor thermal comfort negatively influences urban residents' health and increases residential electricity consumption (REC) for cooling demand. This study adopted the remote sensing-based modified temperature-humidity index (MTHI) to monitor and assess seasonal and spatial characteristics of urban thermal comfort and its association with REC. Thermal comfort and REC have a strong correlation ($p < 0.05$) and the same seasonal patterns as regional climate patterns. Thermal comfort is mainly controlled by land use, land cover (LULC), and physical characteristics of the built environments. Among the physical features, the building height is the most prominent element stimulating thermal discomfort as it regulates other elements linking to urban microclimates, such as sky view factor and ventilation. The thermal comfort in a particular region will be remarkably improved when urban density and building height remain under 65.43% and 17.88 meters, respectively. A green space proportion above 18.9% is also a reference value to optimize thermal comfort in built environments. The most vulnerable regions because of thermal discomfort in the Bangkok Metropolitan Area (BMA) account for 21.4% of the dense urban centers, with a building density of 72.5% and a population density of 17,173 persons/km^2. The research findings enrich the current knowledge of thermal comfort characteristics and REC, which are significantly helpful for regional planning to mitigate thermal discomfort in this megacity.

1. Introduction

Rapid urbanization in the past five decades has gathered more than half of the world's population living in urban settings with considerable transformations in landscapes, socioeconomic structures, lifestyles, and environments (Ritchie and Roser, 2018). Dense population concentration and shifting surface physical characteristics deteriorate outdoor thermal comfort as they directly relate to how open spaces are used (Lai et al., 2019; Quang et al., 2016; Robaa, 2011). Open spaces regulate microclimate factors, which affect the thermal perception of individuals in urban environments, such as temperatures, humidity, wind speed, solar radiation, and even individual experiences. Increasing ambient temperature beyond the thermoneutral zone (i.e., the temperature of the immediate environment in which an individual can maintain normal body temperature with normal basal metabolic rate) can induce low productivity, physiological diseases (e.g., heat stroke, dehydration, and cardiovascular diseases) and psychological health problems for resi-

* Corresponding author. Faculty of Engineering, Prince of Songkla University (Hatyai Campus), Songkhla, 90110, Thailand.
E-mail addresses: trongcan.ng@gmail.com, can.nguyen@czp.cuni.cz (C.T. Nguyen).

https://doi.org/10.1016/j.rsase.2023.101106
Received 10 July 2023; Received in revised form 1 November 2023; Accepted 20 November 2023
Available online 25 November 2023

dents, especially outdoor workers, participants in outdoor activities, and aging residents (Aghamolaei and Lak, 2022; Kumar and Sharma, 2020; Taleghani et al., 2015). These problems are exacerbated by intensive urban expansion, urban heat island effects (UHI), climate change, and prolonged summer days with extreme heatwave episodes.

In essence, indoor thermal comfort is more possibly solvable than outdoor thermal comfort because it can be controlled through building design and technology solutions on a small scale. Therefore, it has received significant attention through the number of studies that were always double as high as outdoor thermal comfort studies (Aghamolaei et al., 2022). In contrast, outdoor thermal comfort is prevailed by larger scale climate and complex interactions between environmental elements. Therefore, outdoor thermal comfort requires integrated urban design and management strategies to effectively improve, such as green infrastructures, shading devices, and water surfaces within urban areas (Nasrollahi et al., 2020; Taleghani, 2018).

In addition to health impacts, the degradation of the urban thermal environment is also associated with building electricity consumption because people rely on air conditioning systems rather than natural ventilation to achieve thermal comfort. They tend to stay longer indoors with air conditioning systems to avoid outdoor thermal discomfort, considerably increasing residential electricity consumption (Kumar and Sharma, 2020). Outdoor urban thermal environment, represented by land surface temperature, has the strongest relationship with residential electricity consumption compared to other sectors (Nguyen et al., 2021b).

It is dubbed as a hot and humid year-round. Thailand and the Bangkok Metropolitan Area (BMA) have experienced extensive urbanization over the past few decades with a noticeable formation of the UHI phenomenon (Keeratikasikorn and Bonafoni, 2018; Khamchiangta and Dhakal, 2020; Nguyen et al., 2022, 2023b; Pan et al., 2023). The more severe thermal environment leads to significant electricity consumption in this region (Arifwidodo and Chandrasiri, 2015; Nguyen et al., 2021b). Specifically, about 26.5% of total electricity consumption comes directly from cooling demand, 65.7% of which serves urban areas (Poolsawat et al., 2020). The city continues to grow as a regional megacity, and the need for electricity in different sectors is likely to increase, which puts pressure on an adequate electricity supply besides ensuring thermal comfort for urban dwellers. Moreover, it is one of the most dynamic and populous areas in Thailand, which is home to 15.2 million inhabitants in 2023 accumulatively (NSO, 2023; WPR, 2023). The proportion of senior residents (over 65 years old) in the BMA is considerably higher than in other regions (NSO, 2023), who are sensitive to extreme temperatures and heatwave episodes (Huang et al., 2018).

Studies on urban heat islands simply consider the severity of temperature, while thermal comfort requires relative humidity (RH) to reveal how people feel to reveal how people feel temperature over a certain RH. Indeed, high RH typically reduces thermal comfort. Spatial investigation on thermal comfort is mainly based on weather data from meteorological stations and reanalysis data, e.g., the universal thermal climate index (UTCI or ERA5-UTCI) (Wu et al., 2019) and temperature humidity index (THI) (Balogun and Daramola, 2019), that often have coarse spatial resolution. Remotely sensed data is promising to provide finer resolution data and better reflect thermal comfort characteristics. Currently, there is rarely a satellite that directly provides information about RH. Feng et al. (2020) proposed the modified THI (MTHI) to replace components of THI with remote sensing data to take advantage of their spatial resolution. Specifically, land surface temperature (LST) and normalized difference moisture index (NDMI) represent temperature and RH, respectively. MTHI can capture critical characteristics of outdoor thermal comfort in many studies and research areas through close relationships between LST versus air temperature and NDMI versus RH. For example, the impacts of landscape patterns on thermal comfort (Feng et al., 2020, 2023) and its spatiotemporal characteristics (Roshan et al., 2022; Yi et al., 2022) were investigated. However, no studies have applied this index to study its relationship to electricity consumption. Landscape patterns influence thermal comfort, but these parameters are abstract and difficult to apply for urban construction planning.

Therefore, this research studied the spatiotemporal fluctuation of MTHI in relationship with residential electricity consumption (REC). It also explores factors affecting thermal comfort and detects their extreme value range, which exacerbates thermal discomfort, as suggestions for urban planning. Finally, we attempted to construct a thermal vulnerability map as a reference map for urban planning to improve thermal comfort in susceptible areas. The research findings with specific spatial and temporal information on thermal comfort and energy consumption are expected to be helpful for the energy sector to provide enough electricity for each area, especially during the hot summer season. The extreme values of factors affecting thermal comfort are considered additional information that needs attention in urban planning in addition to existing construction criteria to improve thermal comfort in vulnerable areas.

2. Methodology

2.1. Study area

The Bangkok Metropolitan Area (BMA) is located in central Thailand. It covers Bangkok and its suburban areas in two contiguous provinces of Samut Prakarn and Nonthaburi (Fig. 1). This region is divided into 18 subregions corresponding to 18 branch offices of the Metropolitan Electricity Authority (MEA) to ensure the electricity supply for each subregion (Can et al., 2021). The BMA belongs to the tropical monsoon humid and is under the influence of the South Asian monsoon regime. Therefore, the regional climate can be distinguished into three seasons: cool and dry winter monsoon (November–February), rainy season (May–October), and local summer (March–April) (Aman et al., 2022; Zhang and Oanh, 2002). The BMA is well-known for its fairly hot year-round, with an average ambient temperature of around 33–38 °C and high relative humidity (~73%) (Arifwidodo and Tanaka, 2015).

2.2. Data collection

2.2.1. Residential electricity consumption (REC)

REC has a significant relationship with urban thermal environment compared to other sectors (Nguyen et al., 2021b). Therefore, it was investigated in this study. The REC data in 2017 was acquired at the Energy Policy and Planning Office (EPPO). The REC is any

Fig. 1. The geographical location of the BMA in central Thailand and regional land use, and land cover delineated from satellite images.

electricity consumption in residential houses, including temples, monks' residences, and establishments. It is a statistically subregional level under the BMA. In essence, the subregional REC depends on the total area and population. Therefore, it should be standardized before further analyses and peer comparison between subregions by estimating the average monthly electricity consumption per person (kWh/person/month). Additionally, the REC is supposed to be unchanged under neutral conditions. We assumed that usage behaviors are relatively stable, and the REC varies mainly originate from seasonal patterns.

2.2.2. MODIS data

Although current studies on thermal comfort use Landsat data with better spatial resolution, it is often influenced by cloud effects, preventing continual observation and comparison with monthly electricity consumption. This study therefore obtained MODIS (Moderate Resolution Imaging Spectroradiometer) data to extract parameters for thermal comfort estimation. Daytime land surface temperature (LST) was obtained from the product (MYD11A2 version 6.1). This is the 8-day composite product at 1000-m resolution. Besides, this research also acquired MODIS surface reflectance product (MYD09A1, version 6.1), which contains visible, near-infrared (NIR), and shortwave infrared (SWIR) bands to analyze surface characteristics. This is also the 8-day composite product with a 500-m resolution. Both two abovementioned products are the products of the Aqua satellite, overpassing at approximately 13:30 local time, which is appropriate to characterize maximum surface temperature (Hulley et al., 2019). These images were overcome a set of preprocessing procedures, including reprojection and quality control, before they were combined into monthly composites. Specifically, the individual pixels were assessed based on the QC band (MYD11A2-LST) and QA band (MYD09A1) to retain only good-quality pixels. The data control procedure assists in eliminating low-quality pixels. However, missing data influences further temporal-spatial analyses. Therefore, these data were then interpolated and smoothed using the Savitzy-Golay filter to impute the missing data and remove potential noises (Fig. 2).

2.2.3. Sentinel-1/2 images

Sentinel-1A time series of VH polarization with a time interval of 15 days was used to enhance the classification capacity of Sentinel-2 optical images, especially for seasonal crops (Diep et al., 2022). A Sentinel-2 yearly image was generated by the median com-

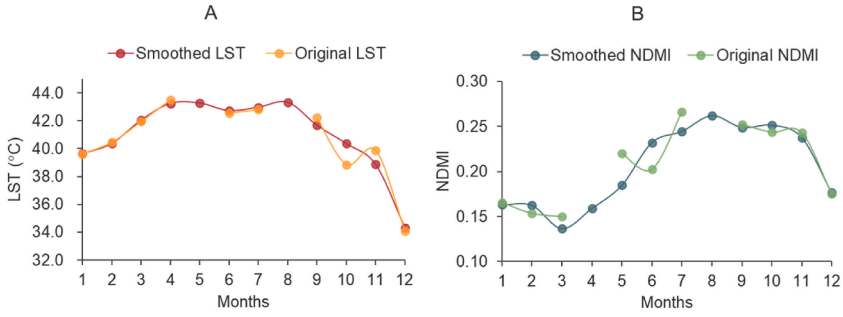

Fig. 2. Data imputation and smooth for (A) LST and (B) normalized difference moisture index (NDMI) time series at a representative pixel. Missing values were efficiently imputed, and abnormal values were adjusted.

posite after removing effects from cloud and cloud shadow pixels. The Sentinel-1 and Sentinel-2 data were combined together for land use, and land cover (LULC) classification (Section 2.3.1). It should be noted that both MODIS and Sentinel-1/2 images are in 2017 to better compare with the available REC data.

2.2.4. Other factors

This research also acquired secondary data and potential factors affecting thermal comfort and vulnerability (Table 1). Land use configuration represented by the proportion of each LULC category mainly controls the urban thermal environment, and it is also expected to influence outdoor thermal comfort (Feng et al., 2020). The LULC proportion for each category was calculated by extracting each class from the LULC map and estimating its ratio for each pixel. Building height was included in the analysis as a critical parameter characterizing vertical characteristics of urban areas against suburban regions, which regulates urban ventilation and ultimately affects thermal comfort (Yi et al., 2022). Meanwhile, population density, to some extent, can reflect urban crowding and the concentration of traffic and transportation as external heat sources (Roshan et al., 2022). Besides, the BMA has a long coastal line in the south, which provides abundant moisture to the city and reduces thermal comfort. Therefore, this study also investigated distance to the coast to explore how it affects thermal comfort.

In addition to the above variables, this study acquired four more variables for thermal vulnerability assessment, which will be clearly described in Section 2.3.5. Specifically, the study considered the sensitive population of younger than 20 years old and older than 65 years old, who are relatively sensitive to extreme thermal conditions (Soebarto et al., 2019; Zhen et al., 2021). Besides, the OSM was acquired to extract three features of parks, cooling facilities, and hospitals and include them in vulnerability assessment as adaption elements. It is a fact that people shelter themselves in public parks to avoid hot weather. The actual cooling centers are not available in Thailand, however, people, especially low-income residents, often visit convenience stores and shopping centers to cool off on torrid days. Finally, distance to hospitals was considered as a backup solution to ensure thermal resilience of the population. For example, when a situation of heat stroke occurs, a person closer to the hospital is assured of timely treatment and better health.

2.3. Methods

This study includes three principal analyses: the relationship between OTC and REC, control factors and optimal ranges, and thermal vulnerability. A detailed description of the main data sources and analytical steps are provided in Fig. 3.

2.3.1. Urban land use, land cover delineation

Urban land use, land cover map was classified by an integrated framework using both optical images from Sentinel-2 and Synthetic-aperture radar (SAR) Sentinel-1A time series. First, the annual composite of the Sentinel-2 image was simply interpreted into three major land cover categories of water bodies, vegetation, and impervious features using unsupervised classification. Subsequently, these three major classes were used as a reference to control the classification scope of the Sentinel-1 time series. Each primary class was classified into multiple subclasses using information from the time series. They were then identified into six LULC categories (i.e., buildings, impervious surfaces, cropland, vegetation, wetland, and water surfaces) based on the major classes and backscatter signals (Fig. 1) (Diep et al., 2022). Finally, the classified LULC map was validated by comparing it to the Copernicus Global Land Service (CGLS) land cover map. The interpreted LULC map achieved high reliability with an overall accuracy of 89.6% (86.6–92.1%, *95% confidence interval*) and a Kappa coefficient of 0.802.

2.3.2. Daytime thermal comfort

Daytime thermal comfort/discomfort is described by the modified temperature-humidity index (MTHI), which facilitates extracting spatial patterns of thermal comfort at finer resolution than other current thermal comfort products. Meanwhile, it still has a high

Table 1
Variables and data sources for control factors analysis and thermal vulnerability assessment.

Variable	Description	Purposes[a]	Data sources**
Building height (BH)	The vertical parameter describes building height (meters)	Re, Tv	Pesaresi and Politis (2022)
Building density (BD)	Proportion of buildings per unit (%)	Re, Tv	LULC
Impervious ratio (IR)	Proportion of impervious surfaces excluding buildings such as roads and pavements (%)	Re	LULC
Cropland density (CRO)	Proportion of cropland per unit (%)	Re	LULC
Vegetation density (VEG)	Proportion of vegetation per unit (%)	Re, Tv	LULC
Wetland density (WET)	Proportion of wetland per unit (%)	Re, Tv	LULC
Water density (WAT)	Proportion of water per unit (%)	Re	LULC
Population density (PD)	Number of population per area unit (persons/km^2)	Re, Tv	WorldPop
Sensitive population (SP)	Sensitive population to thermal discomfort, including infants, young, and senior residents (persons)	Tv	WorldPop
Distance to coast (DC)	Proximity to the coastal line (meters)	Re, Tv	OSM
Distance to parks (DP)	Proximity to the parks (public and residential parks – meters)	Tv	OSM
Distance to cooling facilities (DCC)	Proximity to cooling centers (meters)	Tv	OSM
Distance to hospitals (DH)	Proximity to hospitals (meters)	Tv	OSM

** Data sources: WorldPop: The WorldPop research program (University of Southampton; www.worldpop.org); OSM: Open Street Map.
[a] Purposes: Re = Relationship assessment using Geodetection analysis; Tv = Thermal vulnerability assessment.

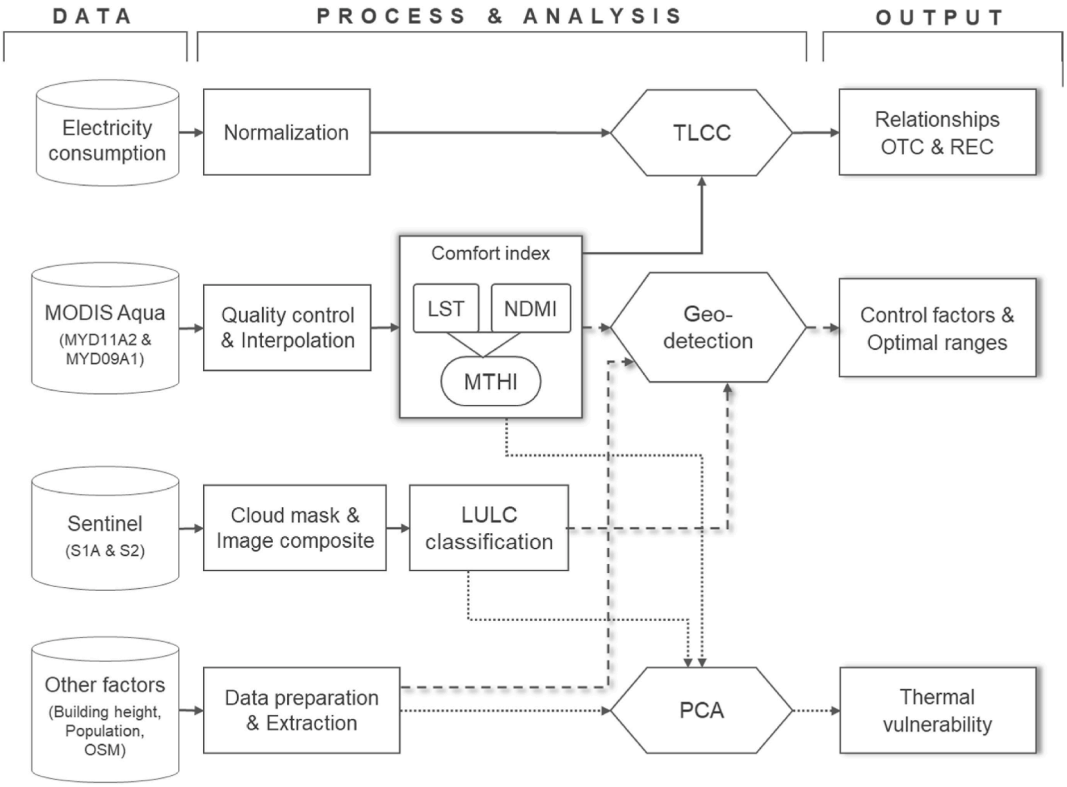

Fig. 3. Methodological framework illustrates data sources, principal analyses, and outputs of this research.

relationship with thermal comfort indices. For instance, the MTHI and ERA5-UTCI (Universal thermal climate index) have a relatively considerable correlation ($r = 0.73$, $p < 0.01$, *it was verified along with this study*). The MTHI represents thermal comfort by considering temperature and humidity to measure the person's experience of how hot a specific temperature is under a corresponding humidity. Specifically, LST and NDMI (normalized difference moisture index) are adopted to represent temperature and humidity, respectively (Feng et al., 2020; Zheng et al., 2022). Even though there is no direct relationship between NDMI and humidity, it potentially captures water content and water vapor related to vegetation (Roshan et al., 2022).

$$MTHI = 1.8 \times LST + 32 - 0.55 \times (1 - 0.01 \times NDMI) \times (1.8 \times LST - 26) \quad (1)$$

$$NDMI = \frac{(NIR - SWIR1)}{(NIR + SWIR1)} \quad (2)$$

where, NIR is the near-infrared wavelength (841–876 nm) and SWIR1 is the shortwave infrared wavelength (1628–1652 nm).

Subsequently, the monthly MTHI values were stretched between [0, 1] for peer comparison between months using maximum and minimum values from all images. Finally, the normalized MTHI was classified into five thermal comfort levels based on global mean and standard deviation values from all standardized images (Yi et al., 2022).

2.3.3. Analyzing relationship between thermal comfort and electricity consumption

The global relationship between monthly REC and normalized MTHI was explored using the Pearson correlation coefficient. Furthermore, the time-lagged cross-correlation (TLCC) was applied to identify the trend of two monthly time series (MTHI and REC). The TLCC incrementally shifts one time series one month step and repeatedly calculates the correlation between two time series to detect whether they move together (i.e., when cross-correlation function (CCF) values reach maxima at $lag = 0$).

2.3.4. Geographical detector analysis

Geographical detection (geodetector) is developed to measure the spatial stratified heterogeneity (SSH) phenomena in spatial datasets, thereby describing their spatial associations and interactions (Wang et al., 2016). Three methods were applied, including factor detection, interaction detection, and risk detection, which identified the significant contributors to thermal comfort, whether or not there is an interaction between them, and the variable value range increasing the severity of thermal discomfort. The factor and interaction detections are measured based on q-statistic, while the risk detection is determined using a *t-test* to compare the mean value between two variable subregions (Wang et al., 2010). Potential thermal comfort contributors vary from LULC proportion to sociodemographic factors (IR, BD, BH, PD, CRO, VEG, WAT, WET, and DC) (Appendix A3). These factors were reclassified into five

classes (i.e., from very low to very high values) by the Jenks Natural Breaks algorithm to maximize the differences among the subclasses (Zhang et al., 2022).

2.3.5. Thermal vulnerability assessment

The thermal vulnerability was synthesized from three critical elements of thermal exposure, sensitivity, and adaptation. Thermal exposure is featured by the MTHI. Thermal sensitivity is a set of factors aggravating thermal discomfort in the city and sensitive factors, including IR, BD, BH, PD, and SP. Besides, thermal adaptation is the measure that contributes to relieving or aiding temperature stress in a city. The elements of thermal adaptation including VEG, WET, DC, DP, DCC, and DH were considered. It should be noted that the density of water, cropland, and impervious surfaces were not considered in the vulnerability assessment because these features have relatively high spatial heterogeneity, which may lead to spatial bias during component analysis (Appendix A3). The variables are disparate in value ranges and units. They therefore have to pass the normalization procedure before the thermal vulnerability assessment. They were then analyzed by the principal component analysis (PCA) to objectively weigh and calculate the individual contribution to ultimate thermal vulnerability (Abrar et al., 2022; Chen et al., 2022).

3. Results

3.1. Spatiotemporal patterns of daytime thermal comfort

The characteristics of daytime thermal comfort were assessed by spatiotemporal patterns of five thermal comfort classes over months (Fig. 4). Its characteristics are closely associated with the regional climate features, which show a high thermal discomfort level during the hot summer (March–June). Over half of the region is dominated by discomfort classes, with the peak achieved in April (71.4%). The thermal comfort gradually improves during the rainy season, which only influences the city center and high-density urban areas. The winter months consistently weakened thermal discomfort for most of the peri-urban. Mainly, no thermal discomfort region was found in December. The spatial distribution of thermal comfort is distinguished through two subregion groups. The urban fringe and coastal subregions (e.g., Bang Buathong, Min Buri, Lat Krabang, Samut Prakarn, Rat Burana, and Bang Plee) experience a more moderate thermal comfort throughout the year compared to other urban subregions (Appendix A1).

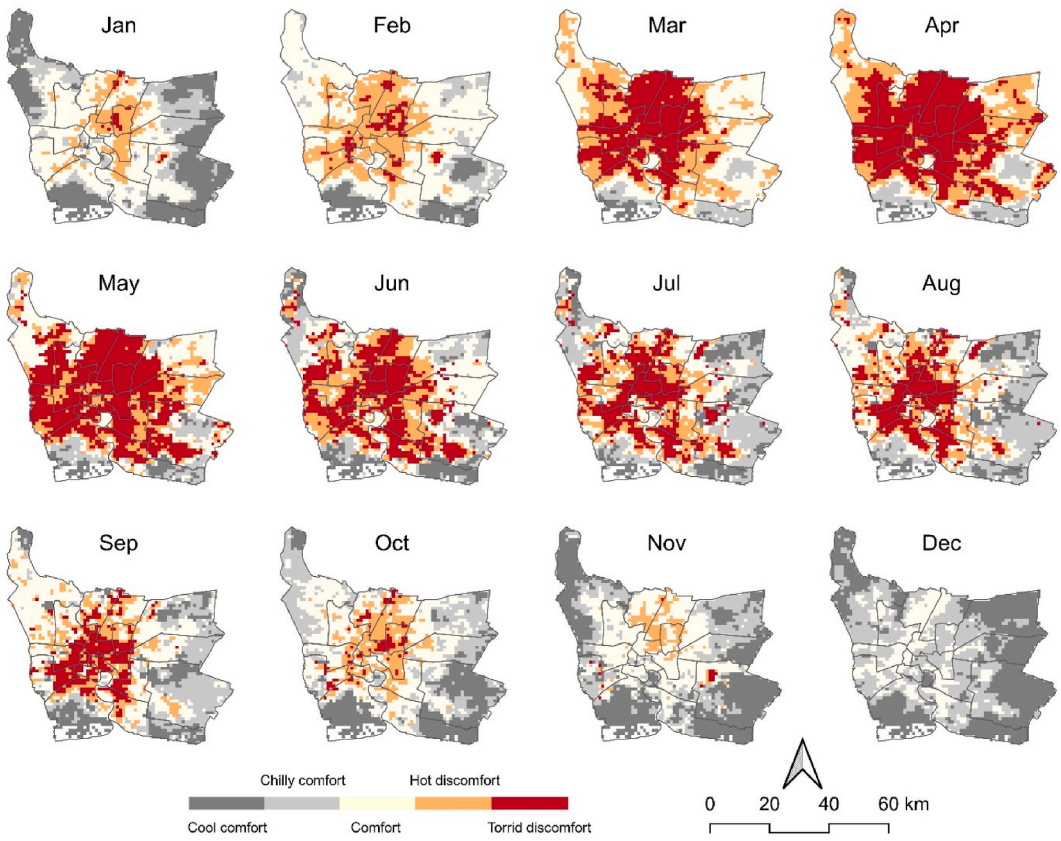

Fig. 4. Daytime thermal comfort categories were classified based on MTHI over months in 2017.

3.2. Residential electricity consumption and relationship with thermal comfort

The monthly residential electricity consumption in the BMA varies between 52.2 kWh/person (Samut Prakarn) and 134.5 kWh/person (Bang Kapi). The peak time for energy consumption is mid-summer, while the winter months are always the off-peak times. The average consumption in the summer months increases by 11.3–14.5% compared to the annual average. It revealed a seasonal pattern of increased electricity consumption due to thermal discomfort, which has a significantly strong correlation with the thermal discomfort index throughout the subregions ($0.66 < r < 0.87$, $p < 0.05$; *Appendix A2*). The peak of electricity consumption occurred during the highest observed thermal discomfort in April. Monthly electricity consumption trends and daytime thermal comfort are parallel over months because CCF (cross-correlation function) values achieve the highest values at the time lag of 0 (Fig. 5). Therefore, the signals of thermal discomfort are supposed to be slightly earlier, to some extent, implying causality impacts of thermal discomfort on increasing electricity usage entire the subregions.

3.3. Interrelationships between thermal comfort and urban environments

The global correlation shows interrelationships among environmental elements and urban thermal comfort, which two clusters apparently depict as influencing manners to thermal comfort (Fig. 6). The negative impact variables comprise green-blue spaces (i.e., WAT, WET, VEG, and CRO). These variables moderately mitigate the severity of thermal discomfort, in which WET contributes a prominent cooling effect with $r = -0.46$ ($p < 0.01$). The distance to the coast represents the cooling effect of sea breeze circulation during the daytime. However, it weakly improves comfort less than 20 km from the coast. In contrast, the urban-related elements

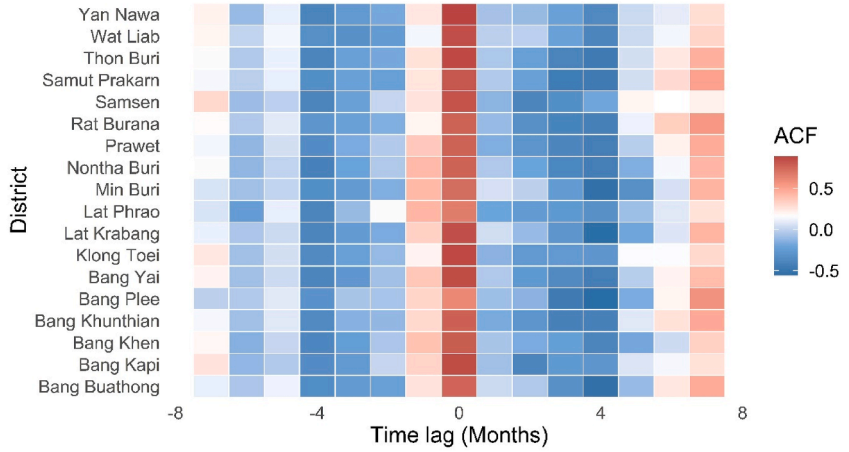

Fig. 5. Time-lagged cross-correlation function (CCF) results between monthly thermal comfort index and electricity consumption at subregion levels.

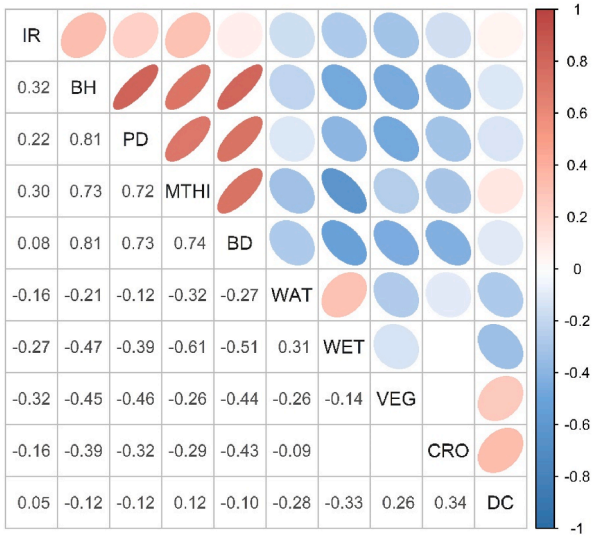

Fig. 6. Correlation matrix between variables. Variables are converged through cluster analysis with significant interrelations. Blank cells eliminate and show insignificant variables ($p > 0.01$).

considerably exacerbate thermal discomfort at a strong significance level ($r > 0.70$, $p < 0.01$). More specifically, population distribution (PD) is closely associated with building density (BD) and building height (BH), which jointly aggravate thermal discomfort.

The geographical heterogeneities of these elements were then explored by geodetector analysis. When spatial characteristics of subregions were considered, the partial effects of CRO, WAT, and IR were revealed to have no significant contribution to thermal comfort/discomfort. The most important contributors are BH > PD > BD > WET ($0.376 < q < 0.485$, $p < 0.001$). The interactions between urban-related factors or with other extreme variables such as coastal proximity (DC) and IR jointly enhance compared to individual impacts ($q > 0.5$). The cool surfaces also interact with each other and improve thermal comfort. These interactions however only reach a relatively weak level ($q < 0.4$). It should be noted that the interactions between them are primarily in nonlinear connections.

Furthermore, minimizing thermal discomfort through MTHI is a key strategy to improve daytime thermal comfort. The theoretical principle is to maximize green-blue spaces while impervious surfaces and urban-related features should be optimized. The risk detection analysis assisted in identifying the thermal discomfort risk under individual impact. Specifically, the daytime thermal discomfort will be intensified mainly in dense urban areas when one or some standards meet or interact within the vulnerable value range (Table 2).

3.4. Thermal vulnerability

The potential factors were analyzed and objectively weighted by PCA, with 68% of the variance explained by the first two components (Appendix A4). Specifically, BH and PD are the two most sensitive factors besides the heat exposure of thermal discomfort. Among adaptive capability factors, hospital and park proximity are the most critical elements increasing resilience against thermal vulnerability. The natural and social characteristics partitioned the BMA area into five levels of thermal vulnerability (Fig. 7). Although the vulnerability considers other elements, it has a considerable correlation with building density ($r = 0.79$, $p < 0.001$). Therefore, the spatial distribution of thermal vulnerability is centralized and gradually decreases along the urban-urban fringe gradi-

Table 2
Urban environment conditions aggravate daytime thermal discomfort corresponding to each variable.

Variable	Description	Value range	Unit	Mean MTHI
IR	Impervious ratio	> 15.99	%	0.767–0.776
BD	Building density	> 65.43	%	0.794
BH	Building height	> 17.88	m	0.792
PD	Population density	> 14,789	person/km^2	0.793
CRO	Proportion of cropland	< 5.04	%	0.778
VEG	Proportion of vegetation	< 18.9	%	0.780
WAT	Proportion of water surfaces	< 4.55	%	0.772
WET	Proportion of wetland	< 5.62	%	0.784
DC	Distance to coast	24.7–49.6	km	0.778

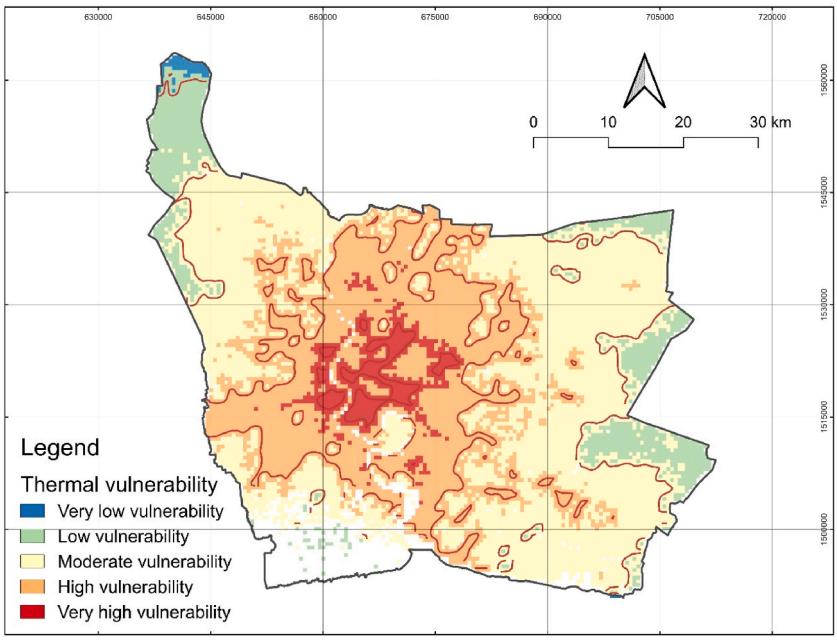

Fig. 7. Thermal vulnerability map over the BMA from synthesized data. Contour lines zoning the core regions for each thermal vulnerability class.

ents. The urban fringes have a very low and low thermal vulnerability, with a total area of about 132 km^2 (4.2%). Next is the area with moderate vulnerability, accounting for nearly 27.8% of the total area, adjacent to the previous regions in the suburban areas. Finally, the high thermal vulnerability is distributed in urban areas with an average building density of 56.4%, which seals 46.6% of the metropolis area. The most vulnerable region is located in the city center and west side of primate city in the populated areas, with a building density of 72.5% and a population of 17,173 persons/km^2.

4. Discussions

4.1. Dependence of thermal comfort on climate pattern and land cover

The physical and social conditions in the built environment are relatively stable within a short period, while thermal comfort varies throughout the year. It is closely associated with seasonal changes in temperature and humidity, i.e., thermal discomfort reaches mid-summer and is relieved during cool winter (Fig. 4). Therefore, thermal discomfort will be exacerbated by extreme climate events such as heatwaves and prolonged drought. We may be exposed to cumulative impacts from thermal discomfort, extreme events, and air pollution episodes, with the same seasonal dependence (Chirasophon and Pochanart, 2020; Kanchanasuta et al., 2020). This increases the adverse effects on human health, especially in the summer.

Besides, outdoor thermal comfort is also governed by land cover features. Although all land cover categories experience fluctuations in the temperature-humidity index over months due to climatic control, they differ in severity. Impervious features (buildings and pavement) and water-related features (water bodies and wetlands) are in turn the most severe and moderate thermal comfort land cover types. Vegetation stands between these two groups, while the MTHI trend of cropland is relatively complex (Fig. 8). It also reaches its highest peak in summer and then significantly decreases during the later seasons. The summer months are the idle period of the main rice crop in Thailand. Therefore, the seasonal bare land amplifies thermal discomfort in rural areas with low impervious surfaces (Cortes and Otadoy, 2020; Nguyen et al., 2021a; Reda and Tripathi, 2016). It increases thermal vulnerability for farmers and outdoor workers. Early warning systems for thermal vulnerability need to be developed, including extreme event forecasting and heatwave episodes, to inform early on thermal discomfort under integrated risks. Economic countermeasures, such as portable cooling systems and cooling vests, should be encouraged and replicated among outdoor workers to increase their thermal comfort (Hamdan et al., 2016; Tang et al., 2021).

4.2. Electricity consumption efficiency

Residential electricity consumption in Thailand is mainly dominated by air conditioning systems, which account for above one-fourth of the total consumption, with low saving potential (Poolsawat et al., 2020). It originates from opening the air conditioner for hours, especially on weekends (Jareemit and Limmeechokchai, 2017). Therefore, the differences in electricity consumption between seasons are caused by climatic patterns and the severity of thermal discomfort. The electricity consumption benchmarking indicates electricity efficiency in subregions, which also depends on the seasonality of thermal comfort (Chaloeytoy et al., 2022). We adjusted the Electricity Use Index (AEUI) by replacing building floor area with building volume—estimated by building footprint and building height data, which reflects how a building volume unit uses electricity per month. The electricity efficiency is relatively low during hot months when residents increasingly use cooling systems. Usually, the inner subregions with high population and high building density have low electricity efficiency. In contrast, the sparse subregions show better electricity efficiency (Fig. 9). In addition to densification of urban features, a high level of outdoor thermal discomfort also partially reduces the electricity efficiency in the inner subregions (Section 3.1 and 3.2).

It should be noted that the urban fringe subregions (e.g., Min Buri, Lat Krabang, and Bang Buathong) are highlighted by their low electricity efficiency. However, they are suburban regions with low population and building density. It can be caused by extensive seasonal cropland areas in these subregions, which increase heat exposure and outdoor thermal discomfort during idle periods and hot season (Fig. 4). At the same time, single houses and villas – the standard housing in these suburban areas, may lead to low electricity efficiency due to the use of single electrical and cooling equipment instead of cooling systems as in the inner city areas. This is an

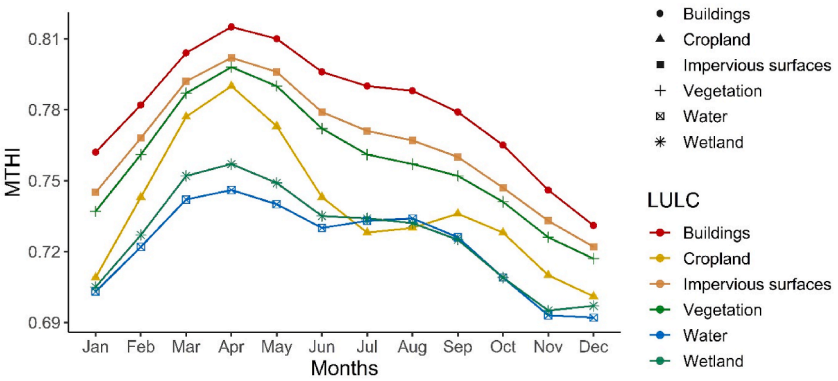

Fig. 8. Temporal changes of MTHI values for different land cover types.

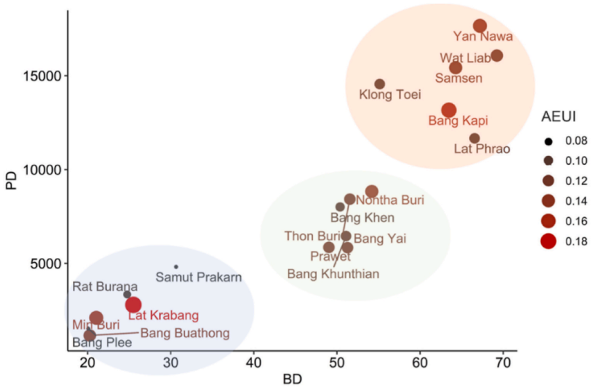

Fig. 9. Scatterplot illustrates relationships between PD, BD, and AEUI. Dot size is proportional to the magnitude of AEUI (Unit: kWh/m3/month). Three groups from the bottom-left correspond to a gradual increase in PD and BD. The lower the AEUI value, the higher the electricity efficiency.

important suggestion to improve electricity efficiency in these suburban districts to prevent energy waste. Simultaneously, appropriate solutions are also needed to improve electricity efficiency in inner urban districts through improving outdoor thermal comfort, where electricity efficiency is currently low.

4.3. Roles of urban green spaces and implication for urban planning

Physical features of the built environment considerably amplify urban thermal comfort and thermal vulnerability compared to other factors. The most prominent element stimulating urban thermal stress is building height (BH), which links to spatial planning (vertical planning) of cities. It regulates other factors and indirectly controls the urban thermal environment, such as sky view factor, urban ventilation, and urban heat island effect (Diem et al., 2023). The high density of tall buildings can exacerbate urban heat islands and thermal discomfort. Urban "vertical expansion" is considered a new urbanization trend to limit horizontal urban overexpansion and optimize the urban transport system and public utilities (Nguyen et al., 2023a). However, the arrangement of zones with different heights should be planned synchronously. Specifically, these research findings suggested reference values for other environmental factors in urban planning to limit extreme thermal discomfort. For example, the building height and density within a particular area should be less than 17.88 meters and 65.43%, respectively, while the vegetation ratio should remain above 18.9% (Table 2).

Wetland significantly relieves thermal discomfort among green-blue spaces because of the double effect of water surfaces and flooded vegetation. It verifies the heat mitigation capacity of wetlands against a unique landscape of vegetation or water bodies. Although vegetation shows lower heat mitigation compared to wetlands, it is prominent as an asset amid a dense and populous city. Urban green spaces, regardless of categories (Fig. 10: public park – A, D, golf courses – B, orchard – C), remarkably reduce thermal vul-

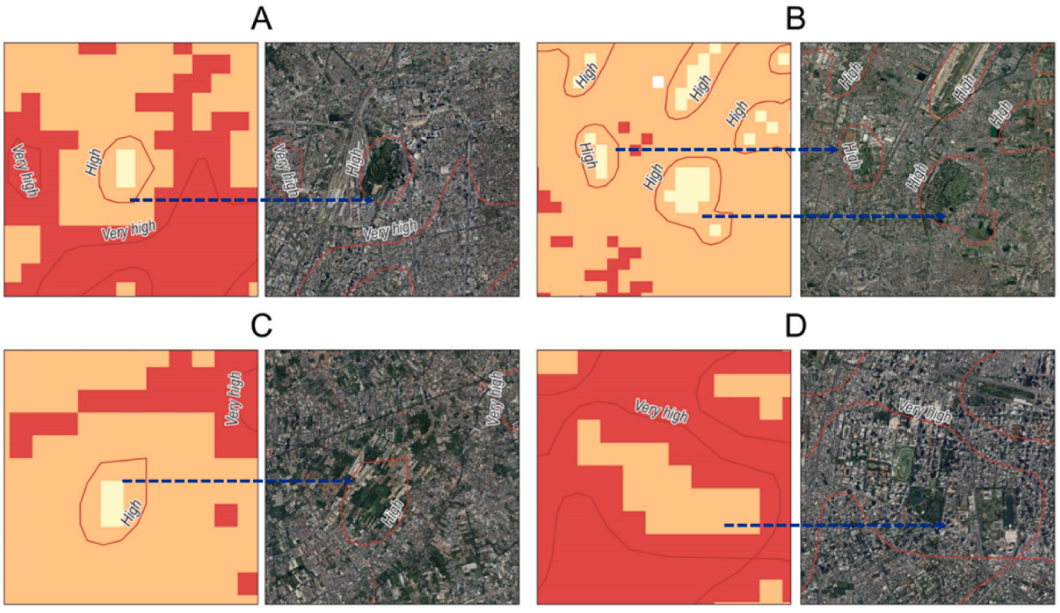

Fig. 10. Zoomed in on thermal vulnerability areas and corresponding landscapes on Google Maps at locations with vast urban green spaces. A, and D are public parks; B is golf courses; and C is orchards.

nerability compared to their vicinities. Therefore, increasing urban green space areas under the Green Bangkok 2030 project will be a potential strategy to improve the city's thermal environment (C40 Cities, 2020). However, it requires joint efforts from public and private stakeholders to jointly push this project to succeed.

In addition, the distance to hospitals and cooling centers is closely related to thermal vulnerability and, at the same time, linked with urban utilities and investment in health care/long-term care, especially when aging tends to be rapid in the future. Hence, the city authority should have a long-term vision to gradually improve the city's thermal resilience when the city is increasingly crowded and vulnerable due to climate change.

4.4. Research limitations and ways forwards

Whilst many studies obtained MTHI from Landsat images to take full advantage of spatial resolution, this study only estimated thermal comfort from MODIS medium resolution images to limit weather effects and monitor monthly progress. The relationships between thermal comfort and electricity consumption have been revealed using these monthly data in the research findinsg. The coarse resolution may lead to noticeable trade-offs. For example, some small scale studies indicated that increasing building height can improve thermal comfort (Chen et al., 2021), while the coarse pixel (~1 km) in this study may not exhibit these characteristics. However, the impact of building height on thermal comfort found in this study is consistent with previous studies based on remote sensing data (Yi et al., 2022). It should be noted that the influences of building height may be complicated and depend on the research scale and specific building height range. Height building provides shading from direct solar radiation, however, it also reduces sky-view factor (SVF) and natural urban ventilation leading to urban heat islands and reduced thermal comfort. Therefore, more studies on the scale effect of building height on thermal comfort deserve to be investigated.

Moreover, the MTHI used in this study was also estimated using the same concept from LST and NDMI. The original proposed index is based on Landsat images. Small differences in image acquisition wavelengths between two satellites can lead to uncertainty. Additionally, the MTHI attempted to modify RH using NDMI, a unitless index that may differ from site to site. The MTHI is estimated from several local normalizations. Therefore, corresponding thermal comfort among study areas is challenging when their thermal comfort indices are estimated separately. It is a note for MTHI users that comparisons between cities and regions should use overall estimates rather than individual calculations.

The residential electricity consumption includes more than forty appliances. Although the electricity usage of other devices may not change over months, there are still potential disparities due to residents' behaviors, building types, building designs, and appliance performance, which representative elements in this study cannot characterize. It is interesting to study how electricity usage behavior changes across months (seasons). It is possible that the cooling (heating) systems are not the only subject to change thereby better providing information for power allocation planning.

5. Conclusion

Spatiotemporal characteristics of outdoor thermal comfort in the BMA were investigated by the remote sensing-based MTHI thermal comfort index, which showed a significant relationship with changes in REC and seasonal solid patterns. The spatial characteristics of urban thermal comfort are closely associated with LULC and physical features of the built environments, while climatic patterns regulate temporal characteristics. These differences in thermal comfort influence residential electricity consumption primarily by air conditioning systems during the hot summer when both thermal discomfort and electricity consumption reach the highest peaks in April.

Geodetection analysis through risk detection identified vital factors influencing thermal comfort. Also, it revealed the value ranges at which thermal comfort begins to deteriorate significantly, e.g., population density, building density, building height, and urban green space proportion, etc. Building height prominently exacerbates urban thermal discomfort because it is closely associated with other urban thermal environment control factors. In contrast, urban green space is a valuable asset to mitigate the thermal stress in cities.

The study also gives geo-oriented information about electricity consumption efficiency and thermal vulnerability, which should have appropriate solutions to improve thermal resilience and electricity efficiency.

Funding

This research receives no external funding.

Ethical statement

Hereby, we consciously assure that for the paper entitled "Seasonal Characteristics of Outdoor Thermal Comfort and Residential Electricity Consumption: A Snapshot in Bangkok Metropolitan Area" the following is fulfilled:

1) This material is the authors' own original work, which has not been previously published elsewhere.
2) The paper is not currently being considered for publication elsewhere.
3) The paper reflects the authors' own research and analysis in a truthful and complete manner.
4) The paper properly credits the meaningful contributions of co-authors and co-researchers.
5) The results are appropriately placed in the context of prior and existing research.
6) All sources used are properly disclosed (correct citation). Literally copying of text must be indicated as such by using quotation marks and giving proper references.

7) All authors have been personally and actively involved in substantial work leading to the paper, and will take public responsibility for its content.

We agree with the above statements and declare that this submission follows the policies of Solid State Ionics as outlined in the Guide for Authors and in the Ethical Statement.

Author statement

Can Trong Nguyen (CTN): conceptualization, methodology, formal analysis, visualization, data curation, writing – original draft, review and editing. Ho Nguyen (HN): writing – review and editing. Anjar Dimara Sakti (ADS): writing – review and editing. All authors have read and approved the submitted work.

Declaration of competing interest

The authors declare that they have no known competing financial interests or personal relationships that could have appeared to influence the work reported in this paper.

Data availability

Data will be made available on request.

Acknowledgment

Authors thank the Metropolitan Electricity Authority (MEA) for the electricity consumption data. Special thanks to Dr. Damrongrit Niammuad and Dr. Rungnapa Kaewthongrach for insightful discussion on the research potential and implications. CTN expresses gratitude to BXT for all kinds of moral support.

Appendix A. Supplementary data

Supplementary data to this article can be found online at https://doi.org/10.1016/j.rsase.2023.101106.

References

Abrar, R., Sarkar, S.K., Nishtha, K.T., Talukdar, S., Shahfahad, Rahman, A., Islam, A.R.M.T., Mosavi, A., 2022. Assessing the spatial mapping of heat vulnerability under urban heat island (UHI) effect in the dhaka metropolitan area. Sustainability 14. https://doi.org/10.3390/su14094945.

Aghamolaei, R., Azizi, M.M., Aminzadeh, B., O'Donnell, J., 2022. A comprehensive review of outdoor thermal comfort in urban areas: effective parameters and approaches. Energy Environ. https://doi.org/10.1177/0958305X221116176.

Aghamolaei, R., Lak, A., 2022. Outdoor thermal comfort for active ageing in urban open spaces: reviewing the concepts and parameters. Ageing Int. https://doi.org/10.1007/s12126-022-09482-w.

Aman, N., Manomaiphiboon, K., Suwattiga, P., Assareh, N., Limpaseni, W., Suwanathada, P., Soonsin, V., Wang, Y., 2022. Visibility, aerosol optical depth, and low-visibility events in Bangkok during the dry season and associated local weather and synoptic patterns. Environ. Monit. Assess. 194. https://doi.org/10.1007/s10661-022-09880-2.

Arifwidodo, S., Chandrasiri, O., 2015. Urban heat island and household energy consumption in Bangkok, Thailand. In: 2015 International Conference on Alternative Energy in Developing Countries and Emerging Economies. Elsevier B.V., pp. 189–194. https://doi.org/10.1016/j.egypro.2015.11.461.

Arifwidodo, S.D., Tanaka, T., 2015. The characteristics of urban heat island in Bangkok, Thailand. Procedia - Soc. Behav. Sci. 195, 423–428. https://doi.org/10.1016/j.sbspro.2015.06.484.

Balogun, I.A., Daramola, M.T., 2019. The outdoor thermal comfort assessment of different urban configurations within Akure City, Nigeria. Urban Clim. 29, 100489. https://doi.org/10.1016/j.uclim.2019.100489.

C40 Cities, 2020. The green Bangkok 2030 project [WWW Document]. URL. https://www.c40.org/case-studies/the-green-bangkok-2030-project/.

Can, N.T., Diep, N.T.H., Iabchoon, S., 2021. Direction of urban expansion in the Bangkok Metropolitan Area, Thailand under the impacts of a national strategy. Vietnam J. Earth Sci. 43. https://doi.org/10.15625/2615-9783/16313.

Chaloeytoy, K., Inkarojrit, V., Thanachareonkit, A., 2022. Electricity consumption in higher education buildings in Thailand during the COVID-19 pandemic. Buildings 12, 1–21. https://doi.org/10.3390/buildings12101532.

Chen, G., Rong, L., Zhang, G., 2021. Unsteady-state CFD simulations on the impacts of urban geometry on outdoor thermal comfort within idealized building arrays. Sustain. Cities Soc. 74, 103187. https://doi.org/10.1016/j.scs.2021.103187.

Chen, T.L., Lin, H., Chiu, Y.H., 2022. Heat vulnerability and extreme heat risk at the metropolitan scale: a case study of Taipei metropolitan area, Taiwan. Urban Clim. 41, 101054. https://doi.org/10.1016/j.uclim.2021.101054.

Chirasophon, S., Pochanart, P., 2020. The long-term characteristics of PM10 and PM2.5 in Bangkok, Thailand. Asian J. Atmos. Environ. 14, 73–83. https://doi.org/10.5572/AJAE.2020.14.1.073.

Cortes, S.T., Otadoy, J.B., 2020. How is climate change shaping food security in Southeast Asia? J. Sci. Eng. Technol. 6, 51–64.

Diem, P.K., Nguyen, C.T., Diem, N.K., Diep, N.T.H., Thao, P.T.B., Hong, T.G., Phan, T.N., 2023. Remote sensing for urban heat island research: progress, current issues, and perspectives. Remote Sens. Appl. Soc. Environ. 101081. https://doi.org/10.1016/j.rsase.2023.101081.

Diep, N.T.H., Loc, H.H., Nguyen, C.T., Park, E., Tran, T., 2022. Spatial-social evaluations of ecosystem services of adaptive aquaculture models using SAR and multivariate analyses: a case in the Vietnamese Mekong Delta. Environ. Monit. Assess. 194, 1–21. https://doi.org/10.1007/s10661-022-10182-w.

Feng, L., Zhao, M., Zhou, Y., Zhu, L., Tian, H., 2020. The seasonal and annual impacts of landscape patterns on the urban thermal comfort using Landsat. Ecol. Indicat. 110, 105798. https://doi.org/10.1016/j.ecolind.2019.105798.

Feng, R., Wang, F., Liu, S., Qi, W., Zhao, Y., Wang, Y., 2023. How urban ecological land affects resident heat exposure: evidence from the mega-urban agglomeration in China. Landsc. Urban Plann. 231, 104643. https://doi.org/10.1016/j.landurbplan.2022.104643.

Hamdan, H., Ghaddar, N., Ouahrani, D., Ghali, K., Itani, M., 2016. PCM cooling vest for improving thermal comfort in hot environment. Int. J. Therm. Sci. 102, 154–167. https://doi.org/10.1016/j.ijthermalsci.2015.12.001.

Huang, C., Cheng, J., Phung, D., Tawatsupa, B., Hu, W., Xu, Z., 2018. Mortality burden attributable to heatwaves in Thailand: a systematic assessment incorporating evidence-based lag structure. Environ. Int. 121, 41–50. https://doi.org/10.1016/j.envint.2018.08.058.

Hulley, G.C., Ghent, D., Frank, M.G., Guillevic, P.C., Mildrexler, D.J., Coll, C., 2019. Land surface temperature. In: Hulley, G.C., Ghent, D. (Eds.), Taking the Temperature of the Earth: Steps towards Integrated Understanding of Variability and Change. Elsevier, pp. 57–127. https://doi.org/10.1016/B978-0-12-814458-

9.00003-4.
Jareemit, D., Limmeechokchai, B., 2017. Understanding resident's perception of energy saving habits in households in Bangkok. Energy Proc. 138, 247–252. https://doi.org/10.1016/j.egypro.2017.10.048.
Kanchanasuta, S., Sooktawee, S., Patpai, A., Vatanasomboon, P., 2020. Temporal variations and potential source areas of fine particulate matter in Bangkok, Thailand. Air Soil. Water Res. 13. https://doi.org/10.1177/1178622120978203.
Keeratikasikorn, C., Bonafoni, S., 2018. Urban heat island analysis over the land use zoning plan of Bangkok by means of Landsat 8 imagery. Rem. Sens. 10. https://doi.org/10.3390/rs10030440.
Khamchiangta, D., Dhakal, S., 2020. Time series analysis of land use and land cover changes related to urban heat island intensity: case of Bangkok Metropolitan Area in Thailand. J. Urban Manag. 9, 383–395. https://doi.org/10.1016/j.jum.2020.09.001.
Kumar, P., Sharma, A., 2020. Study on importance, procedure, and scope of outdoor thermal comfort –A review. Sustain. Cities Soc. 61, 102297. https://doi.org/10.1016/j.scs.2020.102297.
Lai, D., Liu, W., Gan, T., Liu, K., Chen, Q., 2019. A review of mitigating strategies to improve the thermal environment and thermal comfort in urban outdoor spaces. Sci. Total Environ. 661, 337–353. https://doi.org/10.1016/j.scitotenv.2019.01.062.
Nasrollahi, N., Ghosouri, A., Khodakarami, J., Taleghani, M., 2020. Heat-mitigation strategies to improve pedestrian thermal comfort in urban environments: a review. Sustainability 12, 1–23. https://doi.org/10.3390/su122310000.
Nguyen, C.T., Chidthaisong, A., Kaewthongrach, R., Marome, W., 2023a. Urban thermal environment under urban expansion and climate change: a regional perspective from Southeast Asian big cities. In: Ali, Cheshmehzangi, He, Bao-Jie, Ayyoob Sharifi, A.M. (Eds.), Climate Change and Cooling Cities. Springer Nature Singapore, pp. 151–167. https://doi.org/10.1007/978-981-99-3675-5_9.
Nguyen, C.T., Chidthaisong, A., Kieu Diem, P., Huo, L.-Z., 2021a. A modified bare soil index to identify bare land features during agricultural fallow-period in Southeast Asia using Landsat 8. Land 10, 231. https://doi.org/10.3390/land10030231.
Nguyen, C.T., Chidthaisong, A., Limsakul, A., Varnakovida, P., Ekkawatpanit, C., Diem, P.K., Diep, N.T.H., 2022. How do disparate urbanization and climate change imprint on urban thermal variations? A comparison between two dynamic cities in Southeast Asia. Sustain. Cities Soc. 82. https://doi.org/10.1016/j.scs.2022.103882.
Nguyen, C.T., Diep, N.T.H., Diem, P.K., 2021b. Factors affecting urban electricity consumption: a case study in the Bangkok Metropolitan Area using an integrated approach of earth observation data and data analysis. Environ. Sci. Pollut. Res. 28, 12056–12066. https://doi.org/10.1007/s11356-020-09157-6.
Nguyen, C.T., Kaewthongrach, R., Channumsin, S., Chongcheawchamnan, M., Phan, T.N., Niammuad, D., 2023b. A regional assessment of ecological environment quality in Thailand special economic zone: spatial heterogeneous influences and future prediction. Land Degrad. Dev. https://doi.org/10.1002/ldr.4876.
NSO, 2023. Demography Population and Housing Branch. National Statistical Office Thailand (NSO). http://statbbi.nso.go.th/staticreport/page/sector/en/01.aspx. (accessed 27.03.2023).
Pan, L., Lu, L., Fu, P., Nitivattananon, V., Guo, H., 2023. Understanding spatiotemporal evolution of the surface urban heat island in the Bangkok metropolitan region from 2000 to 2020 using enhanced land surface temperature. Geomatics, Nat. Hazards Risk 14. https://doi.org/10.1080/19475705.2023.2174904.
Pesaresi, M., Politis, P., 2022. GHS-BUILT-H R2022A - GHS building height, derived from AW3D30, SRTM30, and Sentinel-2 composite (2018). https://doi.org/10.2905/CE7C0310-9D5E-4AEB-B99E-4755F6062557.
Poolsawat, K., Tachajapong, W., Prasitwattanaseree, S., Wongsapai, W., 2020. Electricity consumption characteristics in Thailand residential sector and its saving potential. Energy Rep. 6, 337–343. https://doi.org/10.1016/j.egyr.2019.11.085.
Quang, D. Van, Kusaka, H., Ho, Q.B., 2016. Impact of future urbanization on temperature and thermal comfort index in a developing tropical city: Ho Chi Minh City. Urban Clim. 17, 20–31. https://doi.org/10.1016/j.uclim.2016.04.003.
Reda, A.G., Tripathi, N.K., 2016. Climate Dynamics and Rice Agriculture in Southeast Asia. OMICS Group eBooks, USA. CA 94404.
Ritchie, H., Roser, M., 2018. Urbanization - Our World in Data.
Robaa, S.M., 2011. Effect of urbanization and industrialization processes on outdoor thermal human comfort in Egypt. Int. J. Meteorol. 36, 111–125. https://doi.org/10.4236/acs.2011.13012.
Roshan, G., Sarli, R., Fitchett, J.M., 2022. Urban heat island and thermal comfort of Esfahan City (Iran) during COVID-19 lockdown. J. Clean. Prod. 352, 131498. https://doi.org/10.1016/j.jclepro.2022.131498.
Soebarto, V., Zhang, H., Schiavon, S., 2019. A thermal comfort environmental chamber study of older and younger people. Build. Environ. 155, 1–14. https://doi.org/10.1016/j.buildenv.2019.03.032.
Taleghani, M., 2018. Outdoor thermal comfort by different heat mitigation strategies- A review. Renew. Sustain. Energy Rev. 81, 2011–2018. https://doi.org/10.1016/j.rser.2017.06.010.
Taleghani, M., Kleerekoper, L., Tenpierik, M., Van Den Dobbelsteen, A., 2015. Outdoor thermal comfort within five different urban forms in the Netherlands. Build. Environ. 83, 65–78. https://doi.org/10.1016/j.buildenv.2014.03.014.
Tang, J., Liu, Y., Du, H., Lan, L., Sun, Y., Wu, J., 2021. The effects of portable cooling systems on thermal comfort and work performance in a hot environment. Build. Simulat. 14, 1667–1683. https://doi.org/10.1007/s12273-021-0766-y.
Wang, J.F., Li, X.H., Christakos, G., Liao, Y.L., Zhang, T., Gu, X., Zheng, X.Y., 2010. Geographical detectors-based health risk assessment and its application in the neural tube defects study of the Heshun Region, China. Int. J. Geogr. Inf. Sci. 24, 107–127. https://doi.org/10.1080/13658810802443457.
Wang, J.F., Zhang, T.L., Fu, B.J., 2016. A measure of spatial stratified heterogeneity. Ecol. Indicat. 67, 250–256. https://doi.org/10.1016/j.ecolind.2016.02.052.
WPR, 2023. World City Populations 2023. World Population Review (WPR). https://worldpopulationreview.com/world-cities/. (accessed 27.03.2023).
Wu, F., Yang, X., Shen, Z., 2019. Regional and seasonal variations of outdoor thermal comfort in China from 1966 to 2016. Sci. Total Environ. 665, 1003–1016. https://doi.org/10.1016/j.scitotenv.2019.02.190.
Yi, T., Wang, H., Liu, C., Li, X., Wu, J., 2022. Thermal comfort differences between urban villages and formal settlements in Chinese developing cities: a case study in Shenzhen. Sci. Total Environ. 853, 158283. https://doi.org/10.1016/j.scitotenv.2022.158283.
Zhang, B.N., Oanh, N.T.K., 2002. Photochemical smog pollution in the Bangkok Metropolitan Region of Thailand in relation to O3 precursor concentrations and meteorological conditions. Atmos. Environ. 36, 4211–4222. https://doi.org/10.1016/S1352-2310(02)00348-5.
Zhang, S., Zhou, Y., Yu, Y., Li, F., Zhang, R., Li, W., 2022. Using the geodetector method to characterize the spatiotemporal dynamics of vegetation and its interaction with environmental factors in the Qinba Mountains, China. Rem. Sens. 14. https://doi.org/10.3390/rs14225794.
Zhen, M., Dong, Q., Chen, P., Ding, W., Zhou, D., Feng, W., 2021. Urban outdoor thermal comfort in western China. J. Asian Architect. Build Eng. 20, 222–236. https://doi.org/10.1080/13467581.2020.1782210.
Zheng, X., Zhang, N., Wang, X., 2022. Development of a modified thermal humidity index and its application to human thermal comfort of urban vegetation patches. Ecosys. Health Sustain. 8, 1–18. https://doi.org/10.1080/20964129.2022.2130095.